

Atmospheric Chemistry of Nonanal

JULIA HURST BOWMAN,[†]
DENNIS J. BARKET, JR.,[†] AND
PAUL B. SHEPSON*^{†,‡}

Department of Chemistry and Department of Earth and
Atmospheric Sciences, Purdue University,
1393 Brown Building, West Lafayette, Indiana 47907

During the Southern Oxidants Study 1999 field campaign at Dickson, TN, we conducted measurements of the *n*-aldehydes propanal, pentanal, hexanal, heptanal, octanal, and nonanal. Propanal and nonanal tended to have the largest concentrations, with afternoon maxima of ~0.3 ppb. These aldehydes typically represented a significant fraction of the VOC reactivity defined as $k_{OH}[VOC]$. However, this information is misleading with regard to the impact of these aldehydes on ozone formation, as their oxidation can represent a significant NO_x sink. Motivated by the relatively large nonanal concentrations, we conducted a laboratory study of the products of the nonanal + OH reaction. The OH + nonanal reaction rate constant was determined via the relative rate technique and found to be $3.6 (\pm 0.7) \times 10^{-11} \text{ cm}^3 \text{ molecule}^{-1} \text{ s}^{-1}$. Under conditions of high [NO₂]/[NO], we determined that $50 \pm 6\%$ of OH-nonanal reaction occurs via abstraction of the aldehydic H-atom through measurement of the peroxyoctyl nitrate yield. We also studied the production of organic nitrates from OH reaction with nonanal in the presence of NO. As expected, a major product (20% at large [NO]/[NO₂]) of this reaction was 1-nitrooxy octane. We calculate that the branching ratio for 1-nitrooxy octane formation from peroxyoctyl radicals is 0.40 ± 0.05 . On the basis of these measurements, we find that for more than 50% of the time OH reacts with nonanal (for midday summer conditions) an organic nitrate or PAN compound is formed, making this important atmospheric aldehyde an effective NO_x sink.

Introduction

It is now well-known (1, 2) that, in rural and forest-impacted regions, isoprene and other biogenic hydrocarbons can be important reactive volatile organic compounds (VOCs). Although the contribution of primary VOCs to tropospheric ozone production has been widely studied (3, 4), less attention has been given to their highly reactive photooxidation products, aldehydes and ketones. Besides being produced from reactions of OH and NO₃ with alkenes (5), aldehydes may be directly emitted from vegetation (6), result from ozonolysis of substances present in the epicuticular wax on plant surfaces (7) and of biogenic fatty acids associated with particulate matter (8), or may arise as primary emissions from combustion sources (9). Yokouchi et al. (10) reported that semivolatile aldehydes are the major reactive VOC components of air samples from a remote location in Japan.

* Corresponding author phone: (765)494-7441; fax: (765)496-2974; e-mail: pshepson@purdue.edu.

[†] Department of Chemistry.

[‡] Department of Earth and Atmospheric Sciences.

Ciccioli et al. (11) found significant concentrations of *n*-aldehydes in both rural and urban areas in Italy. Grosjean et al. (12) found that *n*-aldehydes are present at ppb level concentrations in urban areas of southern California.

Besides participating in tropospheric ozone production, the OH-aldehyde reaction (and aldehyde photolysis) produces free radical species that can combine with NO_x (NO + NO₂) to form organic nitrates or peroxyacyl nitrates (13). These compounds are of great interest because of their ability to transport NO_x over significant distances and supply it to remote areas via their atmospheric degradation. In addition, the organic nitrates produced can serve as a mechanism for the sequestration of odd nitrogen from the atmosphere to be returned via deposition as a forest nutrient (14).

These findings have led us to investigate the abundances of *n*-aldehydes at a rural site in the southern United States and to determine the impact of these species on ozone production. In this paper, we describe findings from the 1999 Southern Oxidants Study (SOS) field campaign as well as the results of photochemical reaction chamber experiments designed to determine the OH reactivity and organic nitrate yields of one of the most important *n*-aldehydes, nonanal (C₈H₁₇CHO).

Experimental Section

SOS Field Campaign. The SOS was established in June 1988 as a multi-year research program to investigate the formation of tropospheric ozone in the U.S. South. The program has included continuous monitoring of regional ozone concentrations, weather and climatic factors, and ozone precursor concentrations in both urban and rural areas of the southeastern United States (15). The Dickson, TN (36°14.82' N, 87°21.85' W), site was designated for the study of rural photochemistry during the SOS 1999 campaign. This area is characterized as a mixed deciduous forest and pastureland, located approximately 53 km WNW of the center of Nashville. Since the typical synoptic flow for this area is from the southwest, Dickson is rarely impacted by the Nashville urban plume; however, the site occasionally receives flow from the direction of TVA's Cumberland (2600 MW capacity) and Johnsonville (1485 MW capacity) power plants, located ~25 km to the northwest and ~50 km southwest of Dickson, respectively.

A series of atmospheric *n*-aldehydes as well as isoprene and its oxidation products was quantitatively determined using an automated Tenax preconcentration and sample injection system driven by Labview 4.1 software (16, 17). Analytes were preconcentrated in a U-shaped trap made of stainless steel tubing (0.470 cm i.d., 0.0770 cm o.d.) and filled with Tenax-TA (2,6-diphenyl-*p*-phenylene oxide) adsorbent, which was held inside the trap by glass frits positioned at each end of the trap. The trap was kept inside an aluminum block containing four cartridge heaters and two tubes through which chilled water was passed for trap cooling. A continuous flow of helium (5 cm³/min) was used to keep the adsorbent clean between sampling periods. The trap was cooled to 5–10 °C as sample air was pumped through at 300 cm³/min. Analyte desorption occurred by heating the Tenax trap to 250 °C under reverse helium flow at 0.88 mL/min and refocusing the analytes in a 30-m PoraPLOT-Q capillary GC column, maintained at an initial temperature of 20 °C. The analytes were then separated using a programmed temperature ramp. A quadrupole mass spectrometer (Hewlett-Packard 5972) with an electron-impact ionization source was used as the detector (mass selective detector or MSD). Detection with the HP MSD was performed in scan mode, from $m/z = 30$

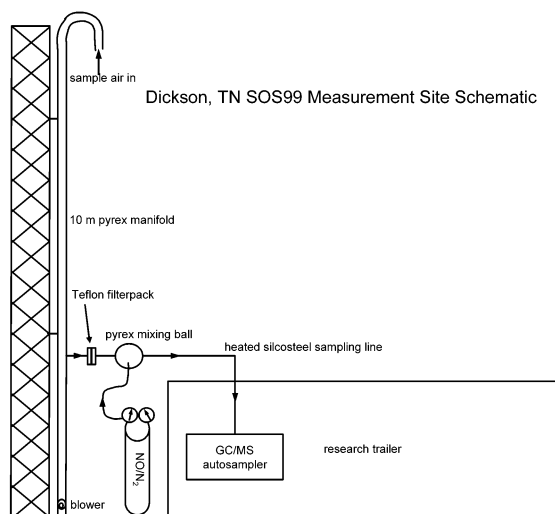
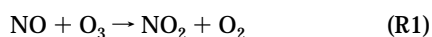


FIGURE 1. Schematic diagram for sampling at the Dickson, TN, SOS99 field site.

to $m/z = 170$. Sample volumes measured using a calibrated mass flow meter (MKS Type 258C) were recorded by the Labview software.

As depicted in Figure 1, the sampling inlet included a Teflon filter for removal of particles, a heated ($100\text{ }^{\circ}\text{C}$) silicosteel line, and a 200-mL glass mixing ball. A 10 mL/min flow of NO (12.4 ppm) was continuously supplied to the glass ball, allowing reaction R1 to take place for removal of ozone:



The diluted concentration of NO (413 ppb) in the mixing ball was chosen such that given the residence time (50 s), for an initial ozone concentration of 80 ppb, ≤ 2 ppt of ozone would reach the Tenax trap (i.e., it is effectively quantitatively removed).

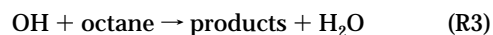
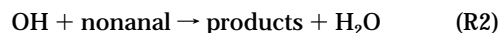
The removal of ozone from the sample is necessary because of potential artifact chemistry, such as reactions that occur on adsorbent traps (18). For example, Roberts et al. (19) reported the appearance of several VOCs on Tenax-GR exposed to 110 ppbv ozone/air mixtures, including hexanal, heptanal, octanal, and nonanal. At present, the mechanism for formation of n -aldehydes on the adsorbents is unknown; it is not possible to produce n -aldehydes directly from O_3 reaction with Tenax itself. We suggest that the n -aldehydes could be formed by the ozonolysis of fatty acids from ambient air that adsorb to unheated sampling lines or that are collected onto the adsorbent. Since in this case ozone is removed and the inlet is filtered and heated, the potential occurrence of such reactions is substantially reduced.

Laboratory Studies. We conducted determinations of the OH–nonanal rate constant and the organic nitrate yield from OH reaction with nonanal, using a 5-m³ all-Teflon photochemical reaction chamber (PRC; 20) fabricated with a PFA-Teflon cylindrical film attached to aluminum end plates coated with PFA-Teflon. The PRC is illuminated with a series of black lamps. A Shimadzu Mini 2 GC with a flame ionization detector (FID) and Hewlett-Packard 3396 series II integrator were used to quantify nonanal concentrations in the PRC. A Gast diaphragm pump was used to sample air at 350 mL/min from the chamber. A (Valco) stainless steel 6-port valve with a 1-cm³ sample loop, which was heated to $150\text{ }^{\circ}\text{C}$, was used to manually switch between sample collection and analysis modes. A Restek RTX 1301(30 m, 0.53 mm i.d.) chromatographic column held isothermally at $100\text{ }^{\circ}\text{C}$ was used for all samples. The stationary phase consisted of a 3.0- μm layer of 6% cyanopropylphenyl and 94% dimethylpolysiloxane.

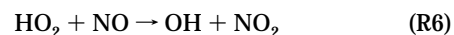
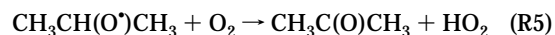
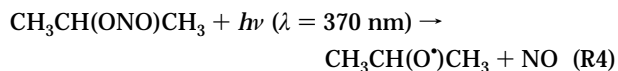
The organic nitrates produced in the PRC were separated and detected using a Hewlett-Packard 5890 GC followed by luminol-chemiluminescence detection. Post-column pyrolysis of organic nitrates produces NO_2 , which is detected in the chemiluminescence reaction vessel of the luminol nitrate detector (LND-4D, Unisearch Associates). The signal produced by the chemiluminescence resulting from reaction of NO_2 and luminol (3-aminophthalhydrazide) (21, 22) was sent to a Hewlett-Packard 3396 series III integrator. The details of this instrumentation are described in Chen et al. (20). Calibration was achieved using isobutyl nitrate (Aldrich) as internal standard during the experiments.

A Thermo Environmental Instruments Company model 42 $\text{NO}/\text{NO}_2/\text{NO}_x$ analyzer was used to measure NO and NO_2 concentrations during experiments. Peroxynonyl nitrate (PNN) was determined using ion chromatography after conversion to nonanoate ion in basic solution (1×10^{-4} M NaOH). The quantitative conversion of peroxyacetyl nitrate to acetate was discussed by Grosjean and Harrison (23). The sample flow rate through the bubblers, bubbler sampling time, final solution volumes, and calibration using nonanoic acid standards were used to determine the PNN concentration. The nonanoate concentrations were corrected for any possible nonanoic acid formation in the PRC, using pure water bubblers (the correction was negligible). The ion chromatographic system was a Dionex DX-500, equipped with an ED40 conductivity detector, GP40 syringe pump, LC25 oven, and an ASRS-ultra (anion self-regenerating suppressor) micromembrane suppressor. The IonPac AG11 guard column and IonPac AS11 analytical column were preceded by an ATC-1 anion trap column for removal of carbonate ions. A 200- μL injection loop was used for sample injection. A 21 mM isocratic NaOH solution was used at 2.0 mL/min for all separations. A stock solution of nonanoic acid in pH 12 NaOH solution was used to generate a calibration curve for nonanoate.

The method of relative rates (24) was used to determine the rate constant for the reaction of nonanal and OH. Octane was chosen as a reference compound because its absolute rate constant has been determined (25) and the Arrhenius expression for this rate constant is well-defined (26) with a room temperature rate constant of $8.72 (\pm 1.7) \times 10^{-12}$ cm³ molecule⁻¹ s⁻¹. A plot of $\ln([\text{nonanal}]_0/[\text{nonanal}]_t)$ vs $\ln([\text{octane}]_0/[\text{octane}]_t)$ yields a straight line with a slope = k_2/k_3 , where k_2 and k_3 refer to the respective rate constants for reactions R2 and R3



(under the conditions of this experiment, the photolysis of nonanal was a negligible loss process). Isopropyl nitrite was used as a source of OH radicals, as shown in reactions R4–R6:



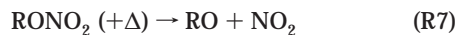
The reaction of nonanal and OH in the presence of NO_x was examined as it occurred in the PRC. Two types of experiments were conducted. The objective of experiment I was determination of the fraction of abstractions that occur from the -CHO group, while the objective of experiment II

was determination of organic nitrate yields from OH reaction with nonanal.

Experiment I. To optimize conditions for production of peroxyxononyl nitrate (PNN; $C_8H_{17}C(O)OONO_2$), the concentration of NO_2 in this experiment was maintained at least 10 times that of NO . Before injecting any compounds into the PRC, samples were taken using the GC/LND, GC/FID, NO_x monitor, and NaOH bubblers. Sample lines were heated to $\sim 80^\circ C$ (except for PNN determination) using heat tape to minimize adsorptive loss. Reactants were injected into the PRC using a glass tee through which clean air was allowed to flow at ~ 2 L/min. Approximately 200 μL of pure nonanal was injected into a heated glass tee using repeated injections with a 10- μL syringe (Hamilton), yielding a final concentration of ~ 1 ppm. A gas sampling bulb and gastight syringe (Hamilton) were used to inject NO_2 . Immediately following injection of NO_2 , concentrations of NO , NO_2 , and NO_x were determined using the NO_x monitor. Isobutyl nitrate (the internal standard) was injected into the glass tee using a high-precision 2- μL syringe (Precision Sampling). Isopropyl nitrite was synthesized in a manner similar to that described by Noyes (27). This compound was injected as a liquid into the PRC as a source of OH radicals, as described above. The impingers were connected to the PRC via a short (~ 20 -cm) PFA-Teflon line, and air was sampled at 500 cm^3/min . The bubbler samples were immediately transferred to presoaked Nalgene bottles before being analyzed using the IC. The bubblers were maintained at $0^\circ C$ during sample collection to enhance the collection efficiency. The PRC was illuminated with black lamps for ~ 2 min periods, followed by sampling for determination of nonanal, organic nitrates, and PNN. The experiments typically involved 4–5 irradiations.

Experiment II. The goal of experiment II was to determine the yields of organic nitrates produced from the OH oxidation of nonanal. This experiment was conducted in a manner similar to experiment I, but with NO in excess, relative to NO_2 . The experiment involved measurement of the concentration of organic nitrate products as a function of the extent of the consumption of nonanal by OH radicals. To inject NO , 7 cm^3 of pure NO at 1 atm was injected into a stream of low-oxygen N_2 flowing through the glass tee using a gastight syringe.

During these experiments, 1-nitrooxy octane ($C_7H_{15}CH_2ONO_2$) was the dominant organic nitrate product detected. To confirm this, 1-nitrooxy octane was synthesized using the method of Ferris et al. (28). The organic nitrates were identified as such in the case of 1-nitrooxy octane by retention time (in comparison to a pure synthesized standard) and for the other organic nitrates by examination of the chromatograms as a function of pyrolyzer temperature. Given the Arrhenius expression (E1) derived from the data of Hiskey et al. (29) for reaction R7:



$$k_7 \cong 1 \times 10^{16} e^{(-20300/T)} s^{-1} \quad (E1)$$

we calculate that at $400^\circ C$ all $RONO_2$ values are quantitatively converted to NO_2 , while at $200^\circ C$, the yield is reduced to 0.3% given the residence time in the pyrolyzer. Thus, for species that are organic nitrates, the peaks disappear in cooling the pyrolyzer from 400 to $200^\circ C$.

Atkinson et al. (30) derived an equation for adjustment of the apparent yields of oxidation products to account for consumption of the product species by OH radicals. Using the experimentally determined rate constant for reaction R2 and estimating the rate constant for the reaction of 1-nitrooxy octane with OH using the method of Kwok and Atkinson (31) ($k = 7.59 \times 10^{-12} cm^3 molecule^{-1} s^{-1}$), the correction factor ranged from 1.01 to 1.03 for 1-nitrooxy octane yield determinations.

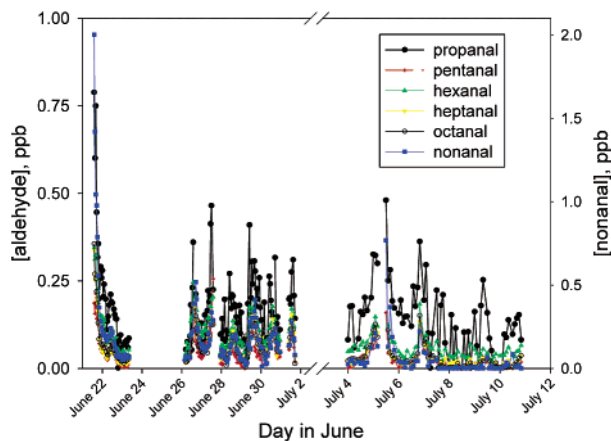


FIGURE 2. SOS 1999 aldehyde data for Dickson, TN.

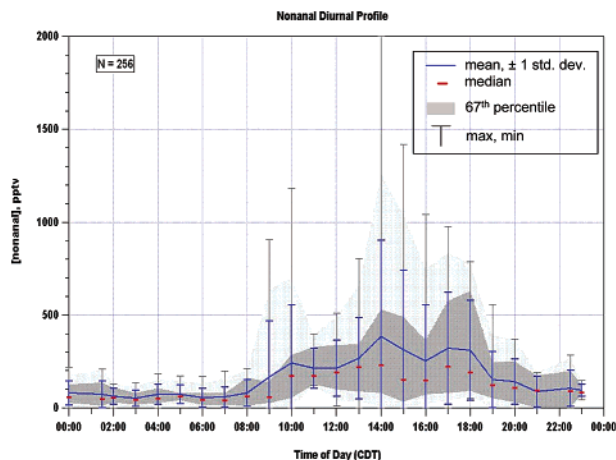


FIGURE 3. Nonanal diel average concentrations for the full measurement period.

In the same manner, an adjustment must be made for loss of PNN via OH radical reaction. The rate constant for this reaction was estimated based on the method of Kwok and Atkinson (31) ($k = 9.23 \times 10^{-12} cm^3 molecule^{-1} s^{-1}$). The range of correction factors (F) in this case was 1.1–1.2.

We also conducted experiments to determine the contribution of wall loss to measurement uncertainties for 1-nitrooxy octane and PNN determinations. Separate wall loss experiments were conducted for both PNN and 1-nitrooxy octane. Wall loss rate constants for these two species were found to be 0.16 and 0.04 h^{-1} , respectively. The product yields were corrected using these rate constants.

Results and Discussion

Ambient Measurements. We conducted quantitative determinations of propanal, pentanal, hexanal, heptanal, octanal, and nonanal at the Dickson, TN, site from June 22 to July 12, 1999. The aldehyde concentrations for three continuous sampling periods are presented in Figure 2. The apparent precision of the GC/MS instrument is demonstrated in the detail available for the n -aldehyde data. As shown in Figure 2, the dominant aldehydes that we measured were propanal and nonanal. Throughout the study, a wide range of aldehyde concentrations was observed with a significant diel cycle typically present. In Figure 3, we present the average nonanal diel cycle obtained by calculating the average concentration within successive 30-min wide time bins over the entire study period. As shown in Figure 3, the average [nonanal] typically varied from a nighttime minimum of ~ 70 ppt to an afternoon maximum of 300–400 ppt. Average

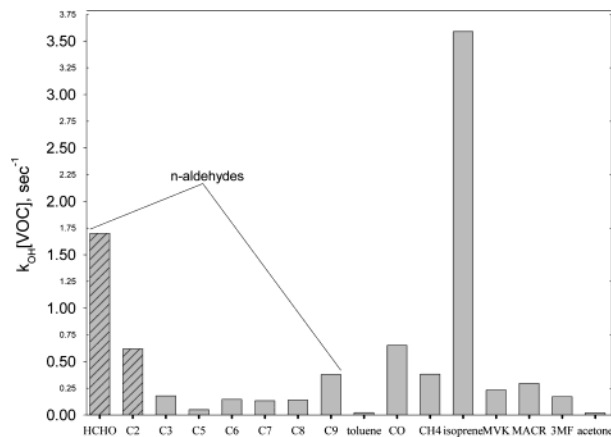


FIGURE 4. OH reactivity for compounds quantified using $t = 1400$ average concentrations. The hatched bars (estimates) represent species not measured in this campaign.

concentrations for *n*-aldehydes at Dickson were as follows: 171, 42, 95, 59, 70, and 198 ppt for propanal, pentanal, hexanal, heptanal, octanal, and nonanal, respectively. These concentrations are comparable to those observed by Yokouchi et al. (10) at Oki Island, who reported nonanal concentrations ranging from ~90 to 900 ppt, but somewhat lower than those observed by Ciccioli et al. (11) in Monti Cimino Forest, who reported concentrations averaging from 300 to 700 ppt.

At the concentrations observed at Dickson, the *n*-aldehydes could have a significant impact on tropospheric chemistry. Specifically, aldehydes are highly reactive toward the OH radical (32). In Figure 4, OH radical reactivities, defined as $k_{OH}[VOC]_i$, for all of the VOC species determined at Dickson are plotted, using the average for the 1400 time frame sample injections. Hydroxyl radical rate constants for propanal, pentanal, and hexanal were experimentally determined by Papagni et al. (33), $k_{OH + nonanal}$ was determined as part of this work (see below), and the remaining *n*-aldehyde rate constants were estimated using the method of Kwok and Atkinson (31). As shown in Figure 4, on average, 12% of the OH reactivity is accounted for by the *n*-aldehydes of $\geq C_3$. Nonanal alone contributes more to OH reactivity than does CH₄, MVK, MACR, or acetone. Since this series includes isoprene, CO, methane, formaldehyde, and acetaldehyde, most of the OH reactivity is likely represented. As data were not available for formaldehyde and acetaldehyde, data from a previous SOS campaign were used as estimates (34) based on relative concentrations.

Given the apparent importance of nonanal and other long-chain aldehydes to VOC reactivity (and as discussed below, as sinks for NO_x), the nature of its sources is important. As discussed above, we believe that the aldehydes measured here do not represent artifact production for at least two reasons: (i) ozone was removed from the inlet and (ii) zero air added to the inlet line did not reveal elevated aldehyde blanks. In addition, laboratory studies were performed to confirm the disappearance of artifact aldehydes with the addition of NO to the mixing ball. However, the possibility of reactions occurring upstream of the mixing ball must also be considered. It is conceivable that the Teflon filter used to remove particulates could provide substantial surface area for ozonolysis of fatty acids present in particulate matter and subsequent release of aldehydes. Correlation plots were constructed to determine the relationship between ozone and the aldehydes; the coefficients (r^2) ranged from 0.3 to 0.44. This relatively weak correlation suggests that some relationship exists, but it does not explain the majority of the variation in the aldehyde data. We find that the diel cycle for nonanal is much stronger than that for O₃. For example,

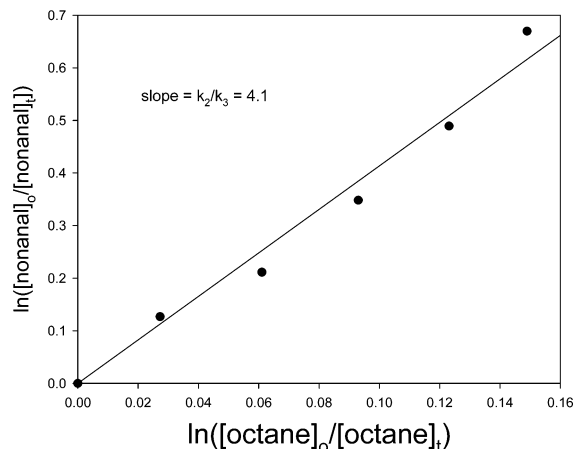


FIGURE 5. Experimental data for one experiment in the relative rate determination of the OH–nonanal rate constant.

during the morning nocturnal inversion breakup, nonanal often increases by several times that of the O₃ increase, implying observed loss of nonanal during the evening (e.g., by dry deposition). In addition, if particulate matter built up on the Teflon filter, then the expected observation would be a steady increase in aldehyde concentrations throughout the study; this was not the case, as shown in Figure 2. It is also the case that we would expect very little nonanal at time zero, with little particulate matter on the filter, which also was not the case. If ozonolysis reactions did take place on the Teflon filter, then it is possible that some portion of our measurement data is artifact; however, this assertion would imply that these reactions can and do take place efficiently in the atmosphere and will contribute to their atmospheric prevalence. This then leads to the need for a better understanding of the atmospheric chemistry of long-chain aldehydes such as nonanal.

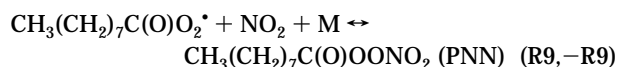
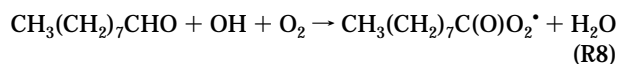
It has become well-known that nonanal (and other long-chain aldehydes) can be produced from the ozonolysis of unsaturated fatty acid lipids (10, 35, 36). As an important example, ozone reacts with oleic acid to produce nonanal and azelaic acid (10, 35). Recent laboratory experiments indicate that this reaction is efficient for O₃ reaction with condensed-phase oleic acid (8). Both oleic acid and azelaic acid have been found to be important constituents of atmospheric particulate matter (35–37). It is also well-known that plant epicuticular waxes contain a multitude of fatty acid lipids (38, 39). The fatty acids can be abraded from leaf surfaces and incorporated into atmospheric particulate matter (40), followed by reaction with O₃ at the particle–atmosphere interface, or they could undergo direct reaction with ozone on the cuticle surface to produce nonanal and other volatile aldehydes. Indeed, it is known that plant epicuticular waxes are commonly present in continental atmospheric particulate matter (41). It thus seems very likely that nonanal and other long-chain aldehydes found in forest environments are produced from ozonolysis of plant lipids, either on the leaf surfaces or on atmospheric particulate matter.

OH–Nonanal Reaction Rate Constant. Given the importance of nonanal chemistry to this type of forest-impacted environment, the kinetics and mechanisms for its atmospheric degradation are important. As the OH radical reaction rate constant (the likely dominant fate for nonanal) is not known, it was determined here in a relative rate experiment. The results for data obtained from a typical experiment are shown in Figure 5, in which $\ln([nonanal]_0/[nonanal]_i)$ is plotted vs $\ln([octane]_0/[octane]_i)$. As shown in Figure 5, the plot is linear with a slope of $4.1 \pm 0.3 = k_2/k_3$. The rate constant for reaction R3, $k_3 = 8.7 \pm 1.7 \times 10^{-12} \text{ cm}^3 \text{ molecule}^{-1} \text{ s}^{-1}$.

Thus, we calculate that the value for $k_2 = 3.6 (\pm 0.7) \times 10^{-11} \text{ cm}^3 \text{ molecule}^{-1} \text{ s}^{-1}$, where the uncertainty is propagated from several component errors but is largely determined from the uncertainty in the slope in Figure 5 and the uncertainty in the published k_3 and reported as a single standard deviation. The method of Kwok and Atkinson (31) leads to calculated OH reaction rate constants of 3.03, 3.17, and $3.30 \times 10^{-11} \text{ cm}^3 \text{ molecule}^{-1} \text{ s}^{-1}$ for heptanal, octanal, and nonanal, respectively. Thus, our measured rate constant is consistent with the semiempirical estimation method.

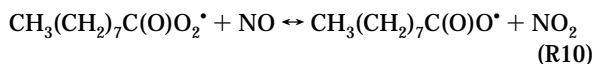
Nonanal–OH Reaction Mechanism. Although the results from Figure 4 imply that nonanal could be an important O_3 precursor, the extent to which that is the case depends on the subsequent RO_2 radical chemistry and the ability of the intermediate radicals to sequester NO_x . As discussed by Arey et al. (42) and O'Brien et al. (43), the yield of organic nitrates for alkyl peroxy and β -hydroxy alkyl peroxy radicals increases with increasing length of the n -alkyl chain. This structural detail results in significantly lower effectiveness for longer-chain hydrocarbons at ozone production than for smaller VOCs with comparable OH reaction rate constants.

Both peroxyacyl nitrates (RC(O)OONO_2) and organic nitrates (RONO_2) may be formed as a result of the oxidation of an n -aldehyde by the OH radical, depending on the position of hydrogen abstraction from the aldehyde. To estimate relative production rates for these species, we can calculate the fractional hydrogen abstraction from the aldehydic position for different n -aldehydes using structure–reactivity relationships (31). For example, the portion of the estimated OH rate constant for propanal that may be attributed to abstraction of the aldehydic hydrogen atom is 95%. Performing a similar calculation for nonanal (reaction R8), we can predict that 63% of hydrogen abstractions occur from the aldehydic position. When OH abstracts the aldehydic H atom, it produces a peroxy nonanyl radical that can remove NO_x as peroxy nonanyl nitrate (PNN), as shown in reaction R9.



The impact of nonanal chemistry on O_3 depends in part on whether OH abstracts the aldehydic H-atom or a methylene H-atom from the alkyl chain (the latter potentially resulting in organic nitrate production). Here we calculate this fraction through experiments discussed below.

Aldehydic Abstraction from Nonanal by OH. The objective of experiment I was to determine the relative rates of abstraction from the aldehydic H-atom versus somewhere on the side chain. This experiment was conducted under conditions of high $[\text{NO}_2]/[\text{NO}]$ to favor reaction R9 over reaction R10:



At sufficiently high $[\text{NO}_2]/[\text{NO}]$, all aldehydic H-atom abstractions lead to production of PNN, and thus quantification of the PNN yield allows determination of the fraction of aldehydic H-atom abstractions. The initial NO_x concentrations were calculated from the volume of gas injected into the chamber (5 mL), taking into account that NO_2 is in equilibrium with N_2O_4 . After each irradiation, NO was measured, and NO_2 was calculated based on that and taking into account the photochemistry. For example, for each molecule of nonanal consumed, a portion of the NO_2 will be lost in the form of PNN (63%). There will also be production

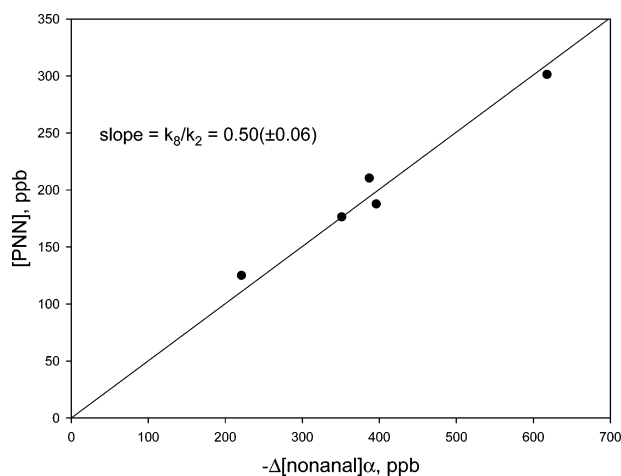


FIGURE 6. Plot of [PNN] vs $-\Delta[\text{nonanal}]\alpha$ for determination of k_8/k_2 .

of NO_2 since the methylene H-atom abstractions produce a peroxy radical that will convert NO to NO_2 (taking into account 1-nitrooxy octane production) and also create an HO_2 radical that will oxidize NO to NO_2 . We also took into account production of NO_x from photolysis of isopropyl nitrite (reactions R4 and R6). During irradiations, these modifications to the NO and NO_2 concentrations were calculated, and these new NO and NO_2 concentrations were used in the calculations below.

The rate of PNN production is given by equation E2:

$$d[\text{PNN}]/dt = k_8[\text{OH}][\text{nonanal}]\alpha \quad (\text{E2})$$

where α is the fraction of peroxy nonanyl radicals that react with NO_2 . Since the total rate of nonanal consumption is $k_2[\text{OH}][\text{nonanal}]$, then we can derive equation E3:

$$\frac{d[\text{PNN}]/dt}{-d[\text{nonanal}]/dt} = \frac{k_8[\text{OH}][\text{nonanal}]\alpha}{k_2[\text{OH}][\text{nonanal}]} = \alpha(k_8/k_2) \quad (\text{E3})$$

Thus, the slope of a plot of $d[\text{PNN}]/dt$ versus $(-d[\text{nonanal}]/dt)\alpha$ is a straight line with slope $= k_8/k_2$. The fraction (α) of peroxy nonanyl (PN) radicals that react to produce PNN (α) was calculated as equation E4:

$$\alpha = R_9/(R_9 + R_{10}) = (1 + (k_{10}/k_9)([\text{NO}]/[\text{NO}_2]))^{-1} \quad (\text{E4})$$

where R represents the reaction rate for the conditions of experiment I, assuming rate constants for reactions R9 and R10 as for peroxyacetyl radicals. Although that is not strictly a valid assumption, it is likely very good for the ratio k_9/k_{10} . This assumption derives in part from the fact that the rate constant for peroxypropionyl radical reaction with NO is very similar to that for peroxyacetyl radicals (44) and that the rate of reaction –R9 is independent of the R group (45), indicating that the bond strength for the O–N bond formed in reaction R9 is independent of the R group. The R group would thus change only the steric factor for reactions R9 and R10 but likely in the same way. The range of values of α derived for experiment I was 90–99%.

In Figure 6, we plot $d[\text{PNN}]/dt$ versus $(-d[\text{nonanal}]/dt)\alpha$. The slope of the plot then is k_8/k_2 or the fraction of abstractions that occur via the aldehydic hydrogen atom. Using α values that correspond to the individual PNN yield points, we obtain a best-fit estimate of $k_8/k_2 = 0.50 \pm 0.06$ (1 s). In addition to reflecting the uncertainty of the slope in Figure 6, the uncertainty expressed here includes the uncertainty in α .

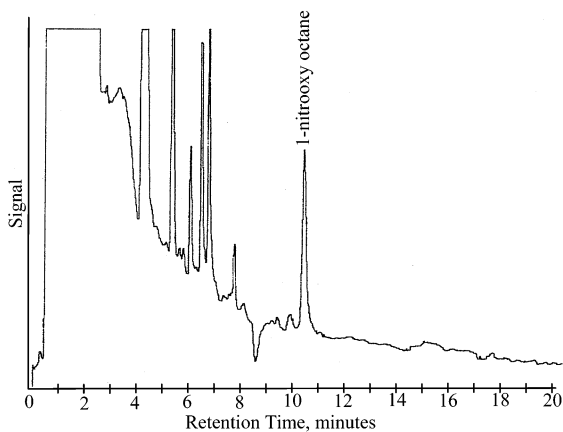
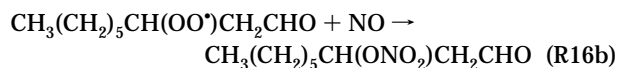
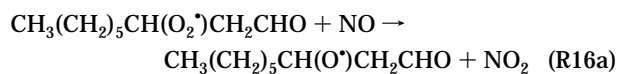
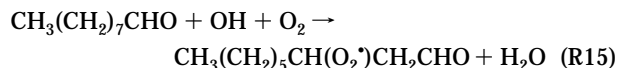
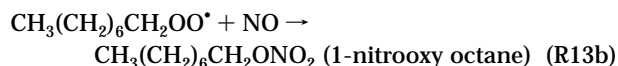
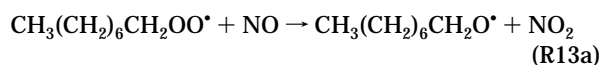
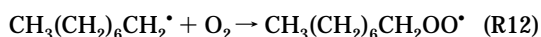
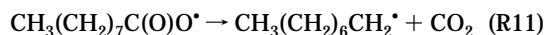


FIGURE 7. Luminol nitrate detector (LND) chromatogram for 1-nitrooxy octane determination.

Organic Nitrate Yields. Under conditions of high [NO]/[NO₂], organic nitrates can be produced as shown in reactions R11–R16:



A representative GC-LND chromatogram for experiment II is shown in Figure 7. Experiment II was conducted to determine the total organic nitrate yield under these conditions. Although the chromatographic conditions were established to afford elution of large semipolar nitrates (1-nitrooxy octane eluted at $t_R = 10.4$ min and $T = 127$ °C; the final column T was 180 °C), only a single organic nitrate was observed under these conditions. Peaks eluting at retention times <9 min represent the internal standard, isobutyl nitrate, isopropyl nitrate (from the isopropyl nitrite), and other products not associated with nonanal. Other small peaks at retention times ranging from 12 to 15 min were occasionally observed, but their individual yields were <1%, indicating that, although they may represent organic nitrate products, their concentrations were below the limit of detection for the LND method and, individually, are much less important than 1-nitrooxy octane.

The rate of production of 1-nitrooxy octane resulting from OH reaction with nonanal is given by equation E5

$$d[\text{1-nitrooxy octane}]/dt = (-d[\text{nonanal}]/dt)\beta\delta\gamma \quad (\text{E5})$$

where β is the fraction of abstractions that occur via the

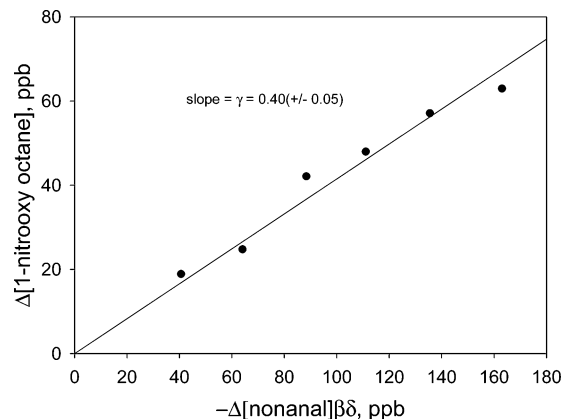


FIGURE 8. 1-Nitrooxy octane branching ratio data.

aldehydic H-atom (i.e., $\beta = k_8/k_2 = 0.50$) to create the PN radical, δ is the fraction of PN radicals that react with NO (calculated assuming the relative rate constants as for R9 and R10 for peroxyacetyl radicals), and $\gamma = k_{13b}/(k_{13a} + k_{13b})$. Thus if we plot $\Delta[1\text{-nitrooxy octane}]$ versus $-\Delta[\text{nonanal}]\beta\delta$, the slope will equal γ . For the conditions of experiment II, $\delta = 1$ at the start of the irradiations. Although some conversion of NO to NO₂ occurs, making the calculated $\delta < 1$, it is effectively equal to 1 throughout the experiment as the small amount of PNN initially formed thermally decomposes (−R9) in the time scale of sampling, followed by reaction R10. The results of four independent determinations of the 1-nitrooxy octane yield during experiment II are shown in Figure 8. The slope of this plot yields $\gamma = 0.40 \pm 0.05$ for peroxyoctyl radicals. The uncertainty of this term includes the calculated uncertainty for β and an estimated uncertainty for δ .

Organic nitrate yields have been determined for *n*-propane to *n*-octane, where the reported total yields reflect the precursor yield-weighted sum of the branching ratios for all isomeric peroxy radicals. From the work of Arey et al. (42), we would predict a total organic nitrate yield for *n*-octane of 0.23. For long-chain alkanes, the primary nitrates are very minor products, as the peroxy radicals are produced from OH reaction with the appropriate alkane and abstraction from the -CH₃ end is minor. Carter and Atkinson (46) reported that the organic nitrate branching ratios for primary peroxy radicals should be scaled by a factor of 0.4 as compared to secondary peroxy radicals; however, it was stated in that work that the primary peroxy radical branching ratio data set is quite limited and relatively uncertain. From the Arey et al. (42) data for a series of alkanes, it is estimated that the branching ratio for organic nitrate production for the secondary peroxy radicals from octane is 0.23. Multiplying this by 0.4 yields an estimated branching ratio for *n*-octyl radicals of 0.09, inconsistent with our determination of 0.40. This result and the recent studies of Espada et al. (47) indicate that there is not, in general, a consistent difference in branching ratios for primary versus secondary peroxy radicals of comparable size. Clearly much more study of the dependence of organic nitrate production as a function peroxy radical structure is necessary.

Atmospheric Implications. As discussed previously, the relative amounts of PNN and 1-nitrooxy octane formed depend on the ratio of NO₂ to NO in a particular environment. Using the NO₂ and NO data from the Dickson site (SOS 1999), the average yields of PNN and 1-nitrooxy octane may be calculated. In addition, using the method of Arey et al. (42), the yield of organic nitrates formed from the carbonyl peroxy radicals (produced from OH abstraction from a -CH₂- on nonanal) may be estimated on the basis of the corresponding alkane, nonane. The sum of the three yields gives the total NO₂ (oxidized nitrogen) species formed as a result of nonanal

Nonanal atmospheric chemistry mechanism

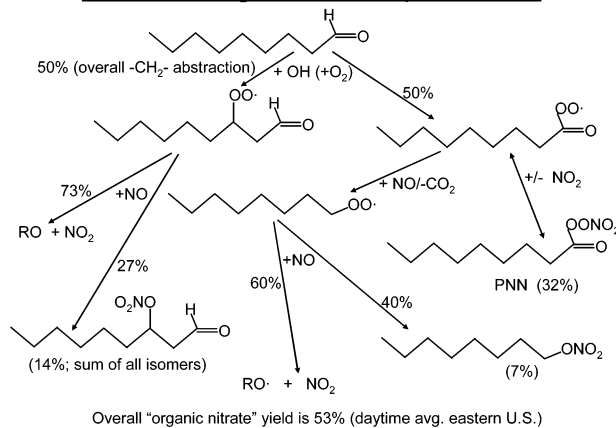
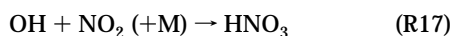


FIGURE 9. Reaction mechanism for conversion of nonanal to organic nitrogen compounds.

oxidation at Dickson. Using equation E4 and the average daytime NO_2/NO at Dickson (3.5), we calculate that 64% of the PN radicals formed will react with NO_2 to make PNN. The remaining fraction (36%) will react with NO to make the 1-octyl peroxy radical. The experimental branching ratio for 1-nitrooxy octane (0.40) represents the fraction of these 1-octyl peroxy radicals that form 1-nitrooxy octane. It follows then that since 50% of nonanal + OH reactions result in formation of the $\text{RC}(\text{O})\text{OO}\cdot$ radicals, $0.50 \times 0.64 = 0.32$ PNN are produced per nonanal oxidized. Furthermore, $0.50 \times (0.36) \times 0.40 = 0.072$ 1-nitrooxy octane are formed per nonanal oxidized. The yield of organic nitrates formed from the carbonyl peroxy radicals is calculated assuming the branching ratios as a function of carbon number determined by Arey et al. (42) applies (i.e., for these C_9 peroxy radicals the branching ratio for organic nitrate formation is estimated to be 0.27). Thus, the carbonyl nitrate yield is this branching ratio times 0.5 (the fraction of abstractions that occur from the side chain) or $0.27 \times 0.5 = 0.14$. We then calculate that the total yield (σ) of organic nitrogen product from OH reaction with nonanal is $\sigma = 0.32 + 0.072 + 0.14 = 0.53$ or, in other words, 53% of the time that OH radicals react with nonanal, radicals and NO_x are consumed. This chemistry is summarized in Figure 9. Thus, nonanal chemistry will have the effect of decreasing atmospheric NO_x and radicals and, consequently, O_3 production rates. Thus the incremental O_3 reactivity for nonanal is likely to be small or negative as expected for aldehydes that efficiently produce peroxyacyl nitrates and/or organic nitrates (48).

This yield in combination with the concentrations of nonanal may be used to calculate the relative importance of nonanal as a sink for NO_x in the boundary layer at Dickson. The formation of HNO_3 (reaction R17) is chosen as a reference as HNO_3 is regarded as the major NO_x sink (49):



The relative rate of formation of NO_x sink compounds from nonanal and HNO_3 may be expressed as follows:

$$\frac{-d[\text{NO}_x] \text{ from nonanal}}{-d[\text{NO}_x] \text{ as HNO}_3} = \frac{k_2[\text{OH}][\text{nonanal}]\sigma}{k_{17}[\text{OH}][\text{NO}_2]} \quad (\text{E6})$$

where $\sigma = 0.53$. On the basis of equation E6, the average daytime conditions at Dickson, nonanal reaction with OH consumes NO_x at 22% the rate of loss via HNO_3 production. These calculations do not take into account the impact of octanal production in reaction R14, which can itself react with OH to begin a new chain oxidation process and similarly act to consume NO_x . It seems likely that organic nitrates of

the type described here, produced from OH oxidation of relatively large biogenic VOC, will contribute significantly to atmospheric NO_z (i.e., oxidized odd nitrogen); indeed these compounds may be a significant part of the "alkyl nitrate" observed by Day et al. (50). Clearly much more work in understanding the sources of long-chain aldehydes and their production in forest-impacted atmospheres is essential to understanding the fate of atmospheric NO_x .

Acknowledgments

We thank the National Oceanic and Atmospheric Administration (which funded our involvement in SOS99) and the National Science Foundation for support of this research (Grant 9816184-ATM).

Literature Cited

- Trainer, M.; Williams, E. J.; Parrish, D. D.; Buhr, M. P.; Allwine, E. J.; Westberg, H.; Fehsenfeld, F. C.; Liu, S. C. *Nature* **1987**, *329*, 705.
- Chameides, W. L.; Fehsenfeld, F.; Rodgers, M. O.; Cardelino, C.; Martinez, J.; Parrish, D. D.; Lonneman, W.; Lawson, D. R.; Rasmussen, R. A.; Zimmerman, P.; Greenberg, J.; Middleton, P.; Wang, T. *J. Geophys. Res.* **1988**, *97*, 6037.
- Friedrich, R.; Obermeier, A. *Reactive Hydrocarbons in the Atmosphere*, Academic Press: San Diego, 1999.
- Frost, G. J.; Trainer, M.; Allwine, G.; Buhr, M. P.; Calvert, J. G.; Cantrell, C. A.; Fehsenfeld, F. C.; Goldan, P. D.; Herwehe, J.; Hhbler, G.; Kuster, W. C.; Martin, R.; McMillen, R. T.; Montzka, S. A.; Norton, R. B.; Parrish, D. D.; Ridley, B. A.; Shetter, R. E.; Walega, J. G.; Watkins, B. A.; Westberg, H. A.; Williams, E. J. *J. Geophys. Res.* **1998**, *103*, 22, 491.
- Atkinson, R. *Atmos. Environ.* **2000**, *34*, 2063.
- Kirstine, W.; Galbally, I.; Yuerong, Y.; Hooper, M. *J. Geophys. Res.* **1995**, *103*, 10, 605.
- Fruekilde, P.; Hjorth, J.; Jensen, N. R.; Kotzia, D.; Larsen, B. *Atmos. Environ.* **1998**, *32*, 1893.
- Moise, T.; Rudich, Y. *J. Phys. Chem. A* **2002**, *106* (27), 6269.
- Graedel, T. E.; Hawkins, D. T.; Claxton, L. D. *Atmospheric Chemical Compounds*; Academic Press: Orlando, FL, 1986.
- Yokouchi, Y.; Mukai, H.; Nakajima, K.; Ambe, Y. *Atmos. Environ.* **1990**, *24*, 439.
- Ciccioli, P.; Brancaleoni, E.; Frattoni, M.; Cecinato, A.; Brachetti, A. *Atmos. Environ.* **1993**, *27A*, 1891.
- Grosjean, E.; Grosjean, D.; Fraser, M. P.; Cass, G. R. *Environ. Sci. Technol.* **1996**, *30*, 2687.
- Roberts, J. M. *Atmos. Environ.* **1990**, *24*, 243.
- Holland, E. A.; Braswell, B. H.; Lamarque, J.-F.; Townsend, A.; Sulzman, J. M.; Müller, J.-F.; Dentener, F.; Brasseur, G.; Levy, H., II; Penner, J. E.; Roelofs, G. J. *Geophys. Res.* **1997**, *102*, 15, 849.
- Meagher, J.; et al. *J. Geophys. Res.* **1998**, *103*, 22, 213.
- Biesenthal, T. A.; Wu, Q.; Shepson, P. B.; Wiebe, H. A.; Anlauf, K. G.; Mackay, G. I. *Atmos. Environ.* **1997**, *31*, 2049.
- Starn, T. K.; Shepson, P. B.; Riemer, D.; Zika, R. G.; Olzyna, K. *J. Geophys. Res.* **1998**, *103*, 22, 437.
- Helmig, D. *Atmos. Environ.* **1997**, *31*, 3635.
- Roberts, J. M.; Fehsenfeld, F. C.; Albritton, D. L.; Sievers, R. E. In *Identification and Analysis of Organic Pollutants in Air*, Keith, L. H., Ed.; Butterworth Publishers: Boston, 1984.
- Chen, X.; Hulbert, D.; Shepson, P. B. *J. Geophys. Res.* **1998**, *103*, 25, 563.
- Maeda, Y.; Aoki, K.; Munemori, M. *Anal. Chem.* **1980**, *52*, 307.
- Wendel, G. J.; Stedman, D. H.; Cantrell, C. A.; Damrauer, L. *Anal. Chem.* **1983**, *55*, 937.
- Grosjean, D.; Harrison, J. *Environ. Sci. Technol.* **1985**, *19*, 749.
- Atkinson, R.; Baulch, D. L.; Cox, R. A.; Hampson, R. F.; Kerr, J. A.; Rossi, M. J.; Troe, J. *J. Phys. Chem. Ref. Data* **1999**, *28*, 191–393.
- Koffend, J. B.; Cohen, N. *Int. J. Chem. Kinet.* **1996**, *28*, 79–87, 1996.
- Atkinson, R. *J. Phys. Chem. Ref. Data* **1997**, *26*, 215.
- Noyes, W. A. *J. Am. Chem. Soc.* **1933**, *55*, 3888.
- Ferris, A. F.; McLean, K. W.; Marks, I. G.; Emmons, W. D. *J. Am. Chem. Soc.* **1953**, *75*, 4078.
- Hiskey, M. A.; Brower, K. R.; Oxley, J. C. *J. Phys. Chem.* **1991**, *95*, 3955–3960.
- Atkinson, R.; Aschmann, S. M.; Carter, W. P.; Winer, A. M.; Pitts, J. N., Jr. *J. Phys. Chem.* **1982**, *86*, 4563.
- Kwok, E. S. C.; Atkinson, R. *Atmos. Environ.* **1995**, *29* (14), 1685.

- (32) Semmes, D. H.; Ravishankara, A. R.; Gump-Perkins, C. A.; Wine, P. H. *Int. J. Chem. Kinet.* **1985**, *17*, 303.
- (33) Papagni, C.; Arey, J.; Atkinson, R. *Int. J. Chem. Kinet.* **2000**, *32* (2), 79.
- (34) Riemer, D. J.; Pos, W.; Milne, P.; Farmer, C.; Zika, R.; Apel, E.; Olszyna, K.; Kliendienst, T.; Lonneman, W.; Bertman, S.; Shepson, P.; Starn, T. *J. Geophys. Res.* **1998**, *103*, 28,111.
- (35) Kawamura, K.; Semere, R.; Imai, Y.; Fujii, Y.; Hayashi, M. *J. Geophys. Res.* **1996**, *101*, 187.
- (36) Limbeck, A.; Puxbaum, H. *Atmos. Environ.* **1999**, *33*, 1847.
- (37) Yokouchi, Y.; Ambe, Y. *Atmos. Environ.* **1986**, *20*, 1727.
- (38) Neinhuis, C.; Koch, K.; Barthlott, W. *Planta* **2001**, *213*, 427.
- (39) Jetter, R.; Schaffer, S. *Plant Physiol.* **2001**, *126*, 1725.
- (40) Rogge, W. F.; Hildemann, L. M.; Mazurek, M. A.; Cass, G. R. *Environ. Sci. Technol.* **1993**, *27*, 2700.
- (41) Conte, M. H.; Weber, J. C. *Nature* **2002**, *417*, 639.
- (42) Arey, J.; Aschmann, S. M.; Kwok, E. S. C.; Atkinson, R. *J. Phys. Chem.* **2001**, *105*, 1020.
- (43) O'Brien, J. M.; Czuba, E.; Hastie, D. R.; Francisco, J. S.; Shepson, P. B. *J. Phys. Chem.* **1998**, *102*, 8903.
- (44) Froyd, K. D.; Lovejoy, E. R. *Int. J. Chem. Kinet.* **1999**, *31*, 221.
- (45) Roberts, J. M.; Bertman, S. B. *Int. J. Chem. Kinet.* **1992**, *24*, 297.
- (46) Carter, W. P. L.; Atkinson, R. *J. Atmos. Chem.* **1989**, *8*, 165.
- (47) Espada, C.; Ford, K.; Grossenbacher, J.; Shepson, P. B. Manuscript to be submitted to *Int. J. Chem. Kinet.*
- (48) Carter, W. P. L. *Atmos. Environ.* **1995**, *29*, 2513.
- (49) Parrish, D. D.; et al. *J. Geophys. Res.* **1993**, *98*, 2927.
- (50) Day, D. A.; Wooldridge, P. J.; Dillon, M. B.; Thornton, J. A.; Cohen, R. C. *J. Geophys. Res.* **2002**, 10.1029/2001JD000779.

Received for review October 8, 2002. Revised manuscript received February 25, 2003. Accepted March 6, 2003.

ES026220P